View metadata, citation and similar papers at core.ac.uk

brought to you by CORE

provided by IntechOpen

We are IntechOpen, the world's leading publisher of Open Access books Built by scientists, for scientists

4,800
Open access books available

122,000
International authors and editors

135M
Downloads

Our authors are among the

154
Countries delivered to

TOP 1%
most cited scientists

12.2%
Contributors from top 500 universities

CLARIVATE ANALYTICS BOOK CITATION INDEX INDEXED

WEB OF SCIENCE™

Selection of our books indexed in the Book Citation Index in Web of Science™ Core Collection (BKCI)

Interested in publishing with us?
Contact book.department@intechopen.com

Numbers displayed above are based on latest data collected.
For more information visit www.intechopen.com

An Illustration of the Effect of Climate Change on the Ocean Wave Climate - A Stochastic Model

Erik Vanem, Bent Natvig, Arne Bang Huseby and Elzbieta M. Bitner-Gregersen

Additional information is available at the end of the chapter

http://dx.doi.org/10.5772/54769

1. Introduction

Rough seas are a major cause for ship losses and significantly contribute to the risk to maritime transportation. It is therefore important to take severe sea state conditions into account, with due treatment of the uncertainties involved, in ship design and operation. There is thus a need for appropriate stochastic models describing the variability of sea states and these should also consider long-term trends related to climate change. This chapter presents such a stochastic model, aiming at describing the spatial and temporal variability, as well as long-term trends, in the ocean wave climate.

The stochastic ocean wave model presented in this chapter exploits the flexible framework of Bayesian hierarchical space-time models. It allows modelling of complex dependence structures in space and time and incorporation of physical features and prior knowledge, yet at the same time remains intuitive and easily interpreted. Furthermore, by taking a Bayesian approach, the uncertainties of the model parameters are also taken into account. Different alternatives for modelling the long-term trend are suggested, with and without a regression component with CO_2 as an explanatory variable. The models have been fitted by monthly maximum significant wave height data for an area in the North Atlantic ocean. The different components of the model will be outlined in this chapter, and the results will be discussed. Furthermore, the influence of the estimated expected long-term trends on the environmental loads of ocean-going ships will be investigated.

According to the Intergovernmental Panel of Climate Change (IPCC) [21–23], the globe is experiencing climate change. The IPCC report [21] also presents projections of future climate change, and it is deemed very likely that frequencies and intensities of some extreme weather events will increase. However, a more recent summary report is more careful in its conclusions [23].

Ships and other marine structures are constantly exposed to the wave and wind forces of its environment, and extreme ocean climate represents a risk to marine operations. Bad weather

INTECH
open science | open minds

© 2013 Vanem et al., licensee InTech. This is an open access chapter distributed under the terms of the Creative Commons Attribution License (http://creativecommons.org/licenses/by/3.0), which permits unrestricted use, distribution, and reproduction in any medium, provided the original work is properly cited.

is indeed often involved in accidents and ship losses, and this stresses the importance of taking extreme sea state conditions adequately into account in ship design. This is important to ensure that the ships can withstand the environmental forces they are expected to encounter throughout their lifetime. Hence, a correct and thorough understanding of meteorological and oceanographic conditions and the extreme values of relevant wave and wind parameters, in particular wave parameters such as the significant wave height (H_s) is of paramount importance to maritime safety, and there is a need for appropriate statistical models to describe the variability of these phenomena. Long-term statistics can then be combined with individual wave statistics in order to estimate the highest waves that should be used in design of marine structures, as outlined in e.g. [1].

In particular, with the observed and projected climate change that the globe is currently experiencing, it may no longer be sufficient to base design codes and safety standards on current knowledge about the past and present ocean environment. The implicit assumption that the future will be like the past may no longer be even approximately valid and there is a need to consider how wave parameters are expected to change in the future, as a consequence of climate change. Thus, there is a need for time-dependent statistical models that can take the long-term time-dependency of integrated wave parameters properly into account.

In this chapter, a Bayesian hierarchical space-time model ([46], [47]) will be outlined that has been developed to describe significant wave height as a stochastic spatio-temporal process ([37]). The model is hierarchical and allows for modelling of complex dependence structures in space and time and includes prior information by way of informative priors. It is built up by different components including a purely spatial field, a short-term, spatio-temporal dynamic component, a temporal seasonal component, and finally, a separate term for modelling long-term trends, possibly as a consequence of climate change. The model has been fitted to significant wave height data for an area in the North Atlantic ocean, selected because North Atlantic conditions are used as design basis for the majority of sailing ships. The selection of the modelling approach was based on a thorough literature survey, presented in [35]. Bayesian hierarchical space-time models are also treated in the book [13].

The model and its various components will be outlined in a subsequent section. Furthermore, different variations and extensions to the main model will be introduced. Most importantly, a logarithmic transform of the data yields a different interpretation of the model ([39]) and the long-term trend component will be modelled as a regression block, where the trends in significant wave height are regressed on levels of atmospheric CO_2 ([38]). In this way, long-term trends in the data are identified, and projections of future ocean wave climate can be made based on different emission scenarios.

Finally, it is demonstrated how the estimated expected increase in severity of future ocean wave climate is related to the structural loads and responses of ships at sea and how these effects can be taken into account in load calculations ([36]). It was found that the models predict a non-negligible effect on the extreme environmental loads. Hence, the findings indicate that the effect of climate change on the ocean wave climate may need to be considered in ship and marine structures design.

2. Description of location

The scope of this study is restricted to consider an area in the North Atlantic ocean, i.e. the ocean area between 51°-63° north and 12°-36° west (or 324°-348° east). The spatial resolution of the data is $1.5° \times 1.5°$, hence a grid of 9 x 17 = 153 datapoints covers the area. It is noted that due to the curvature of the surface of the earth, the distance between gridpoints will not be constant throughout the area. The distance in the north-south direction is fairly constant but the distance in the longitudinal direction (east-west) differs significantly for different latitudes. However, in the following analysis of spatial variability, this fact will be ignored. The area under consideration is illustrated on a map in figure 1.

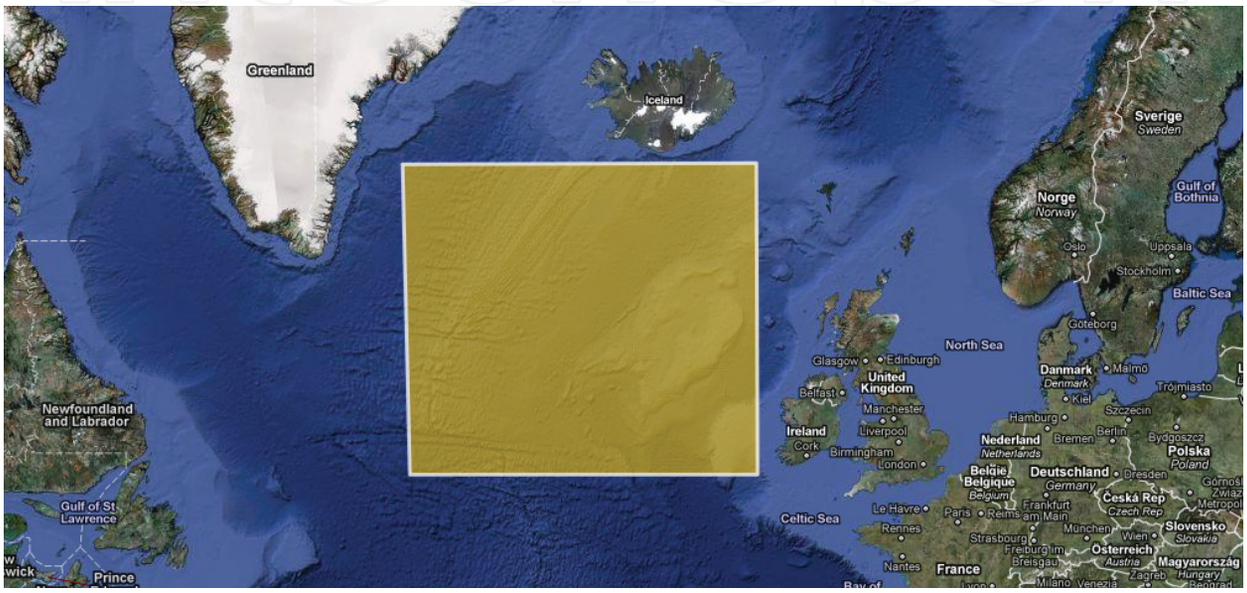

Figure 1. The area of the North Atlantic ocean under consideration

3. Description of data

Data for significant wave height have been used to fit the stochastic model, and data on levels of CO_2 concentrations in the atmosphere have been used as covariates. In the following, a brief description of these sets of data will be given.

3.1. Wave data

The reanalysis project ERA-40 [34] was carried out by the European Centre for Medium-Range Weather Forecasts (ECMWF) and covers the 45-year period from September 1957 to August 2002. Data obtained from this reanalysis include six-hourly sampled global fields of significant wave height; global, continuous data are available on a 1.5° x 1.5° grid, making this perhaps the most complete wave dataset available to date.

It has been reported that the ERA-40 dataset contains some limitations which indicate problems in using these data for modelling long-term trends in extreme waves ([32]). However, corrected datasets for the significant wave height have been produced, resulting in a new 45-year global six-hourly dataset of significant wave height ([10]). When compared

to buoy measurement and global altimeter data, this corrected dataset, referred to as the C-ERA-40 data, shows clear improvements compared to the original data ([11]). It is this corrected dataset, which was kindly provided by the Royal Netherlands Meteorological Institute (KNMI)[1] that has been used in this study. It includes fields of significant wave height sampled every 6th hour with a spatial resolution of $1.5^\circ \times 1.5^\circ$ covering the period from January 1958 to February 2002 (i.e. a total of 44 years and 2 months which corresponds to a sequence of 64 520 points in time). However, for this particular study it is deemed sufficient to use monthly maximum data at each location, totalling 530 monthly maxima in time for each location.

In general, it is acknowledged that wave buoys are regarded as highly accurate instruments, and it is stated in e.g. [7] that both the systematic and random error of significant wave height measurements by buoys are negligible. However, when calibrating hindcast data against observations, the data will still be subject to epistemic uncertainty due to the way the calibration is carried out and high values of significant wave height will normally be more affected by uncertainties, as discussed in [6]. For the purpose of this study it is emphasized that all modelling and all results are conditional on the input data and data validation and data uncertainty is considered out of scope.

3.2. CO_2 data

Concentrations of atmospheric CO_2 have been used as covariates for explaining possible long-term trends in the significant wave height, and basically two sets of data have been exploited; historic data for model fitting and projections of future concentration levels for future predictions.

3.2.1. Historic CO_2 data

The aim of introducing a regression component with CO_2 levels as covariates is to identify long-term trends, and it is deemed sufficient to use monthly data. Hence, monthly average CO_2 data from the Mauna Loa Observatory, Hawaii, have been used ([33]). The data are on the format of the number of molecules of carbon dioxide divided by the number of molecules of dry air multiplied by one million (parts per million = ppm), and data are available from March 1958 to present. The data set contains the monthly averages determined from daily averages, as well as interpolated monthly averages where missing data have been replaced by interpolated values. Finally, monthly trend values are given where the seasonal cycle has been removed and where linear interpolation has been used for missing months. For the purpose of this study, the monthly trend time series will be used as covariates for the long term trend. The seasonal cycle in the monthly maximum significant wave height is accounted for in a separate seasonal component in the model.

The monthly interpolated and trend data are illustrated in the graphs in figure 2 and the vertical lines represent the part of the time series that overlap the C-ERA-40 data for significant wave height. It is noted that the CO_2 data starts at March 1958 whereas the significant wave

[1] Private communication with Dr. Andreas Sterl, KNMI

height data starts at January 1958. Therefore, when utilizing the CO_2 data, the model will be run with data starting at January 1959.

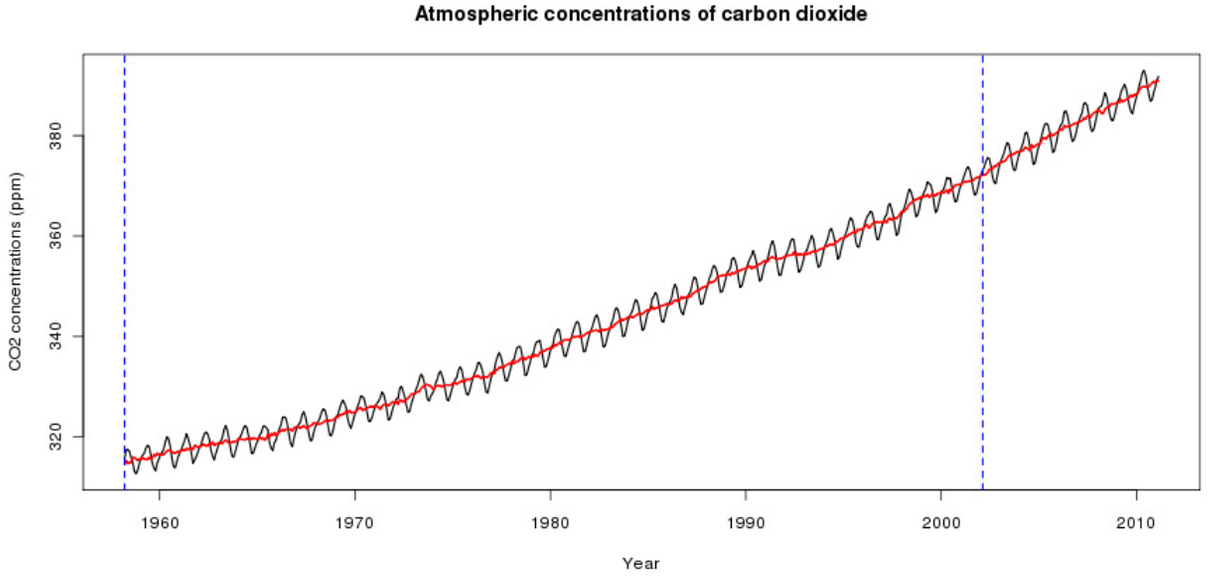

Figure 2. CO_2 data from the Mauna Loa Observatory, monthly interpolated data (black line) and trend data with seasonal effects removed (red lines)

It is acknowledged that CO_2 is just one greenhouse gas (GHG) and that it does not alone determine the radiative forcing of the globe; other important GHGs are for example methane (CH_4) and nitrous oxide (N_2O). Nevertheless, it is generally agreed that CO_2 is the most important GHG and for the purpose of this study, it is construed as a proxy for the concentration of GHG in the atmosphere. More sophisticated models could include other GHGs and aerosols as covariates as well. It is also noted that the data stem from observations outside of the area in the North Atlantic which is the focus of this study. However, it is assumed that CO_2 is well mixed in the atmosphere, and that this does not introduce any notable bias in the results pertaining to expected long-term trends.

3.2.2. Future projections of CO_2 levels

Future projections of the atmospheric concentration of CO_2 will be exploited to make projections of future wave climate. Future predictions are inevitably uncertain, and different projections of CO_2 levels have been made based on different emission scenarios ([27]). Projected emissions and concentrations presented by IPCC for the four marker scenarios A1B, A2, B1 and B2 have been considered[2]. The scenarios A2 and B1 correspond to the highest and lowest projected CO_2 levels respectively, and it is therefore assumed sufficient to employ these two in the modelling. Scenario A2 might be an extreme scenario, but from a precautionary perspective it is important to concider since this could be construed as a worst case scenario. The CO_2 projections data can also be found in appendix II of [20].

[2] The IPCC Data Distribution Centre, URL: http://www.ipcc-data.org/ddc_co2.html

The projected levels of atmospheric CO_2 concentrations are given for every ten year towards 2100. For the purpose of this study, monthly averages are needed, and simple linear interpolation within each decade has been used to estimate monthly projections. The decadal projections are then assumed as the value for January of that year. In this way, monthly projections of CO_2 levels in the atmosphere from year 2010 until 2100 is obtained for use as covariates. For the years 2002 to 2010, where actual observations are available, recorded monthly averages from the Mauna Loa Observatory will be used. The interpolated monthly projections are plotted together with the original decadal projections in figure 3 (the vertical bars in the plots correspond to the decadal reference projections from the ISAM model ([24])).

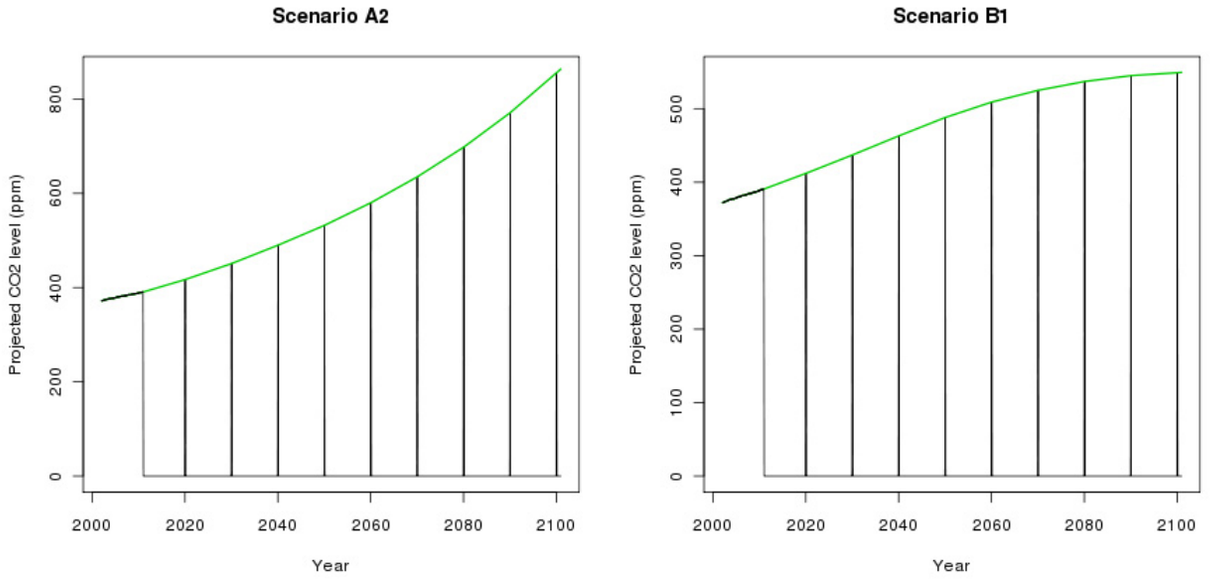

Figure 3. Interpolated monthly CO_2 level projections for scenarios A2 and B1

The uncertainty of the data is not accounted for and any results are also conditional on the data used for the covariates. Uncertainties are of course large for future predictions, but it is assumed that the projections suggested by the IPCC correspond to the best current knowledge available. The uncertainties of future projections of CO_2 concentrations were discussed in e.g. [25] and it was suggested to assign probabilities for the various scenarios. However, such probabilities have not been assigned in this study. The historic data and the projections corresponding to the four marker scenarios are illustrated together in figure 4.

4. Initial inspection of the wave data

The density of all the monthly maxima is shown in figure 5 and two distinct modes can be identified, one around 5 meters and another at about 8 meters. It is believed that these correspond to different characteristics during calm and rough seasons. For the whole dataset, the mean monthly maximum is 7.5 meters, and the average monthly maxima for each month are given in table 1. Density plots (not shown) for each month show that the months January - March and October-December have peaks around 8-9 meters and that the months May-August have peaks around 5 meters. The remaining months, April and September are

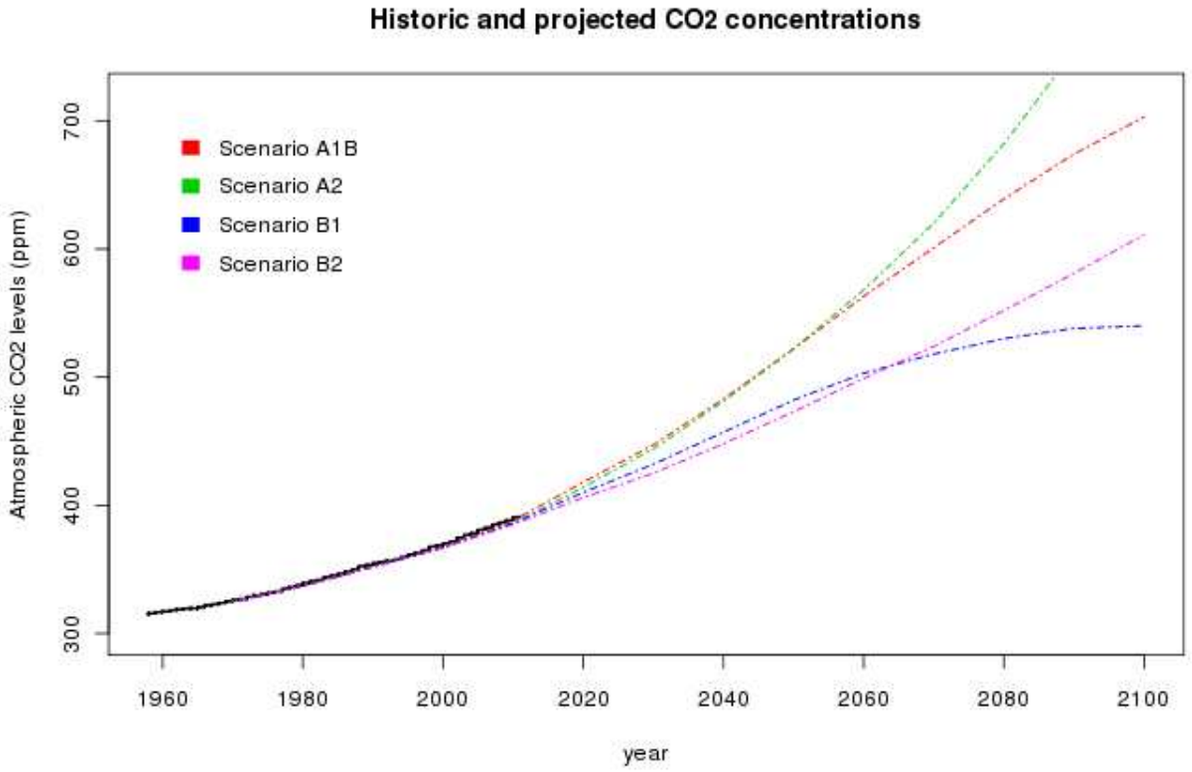

Figure 4. Atmospheric CO_2 levels: Historic data and future projections

more flat with most probability mass between 5 and 8 meters. At any rate, the two modes in the density plot seem to be explained by the peaks at the different months.

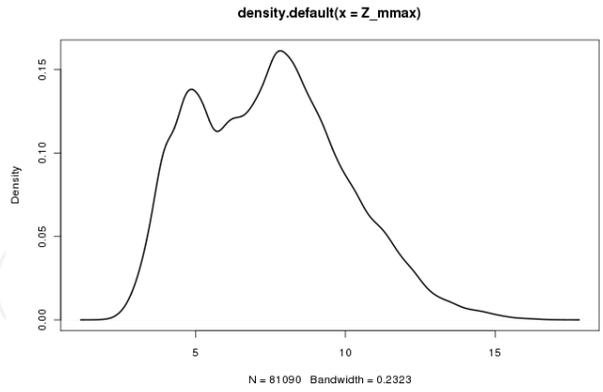

Figure 5. The density of the monthly maximum data

Jan	Feb	Mar	Apr	May	Jun	Jul	Aug	Sep	Oct	Nov	Dec
9.87	9.63	8.91	7.18	5.89	5.03	4.42	5.04	6.96	8.21	8.69	9.79

Table 1. Average monthly maxima for each month

One may also check for normality or log-normality, but tests show that the data are neither Gaussian nor log-normal. Furthermore, attempts to describe the spatial and temporal variability by simple regression and autocorrelation models fail. Hence, it is apparent that the

data cannot be well described by simple models and a somewhat more sophisticated model must be constructed. Hierarchical models are known to model spatio-temporal processes with complex dependence structures at different scales [45]. Therefore, a Bayesian hierarchical space-time model, along the lines drawn out by e.g. [46] will be constructed to model the significant waveheight data in space and time.

4.1. Logarithmic transformation of the data

Higher wave heights are normally associated with higher uncertainty (noise), and heteroscedastic features are observed in the significant wave height data. One way to account for such heteroscedasticity could be to take the log-transform of the data. Furthermore, taking the log-transform of the data yields a fundamentally different interpretation of the contributions from the various model components, which become multiplicative rather than additive. Hence, a revised model would associate higher trends with extreme sea states compared to non-extremes. It is noted that for inference made on log-transformed data, biases may be introduced when re-transforming back to the original scale. Bias correction factors and how to deal with the re-transformation bias are discussed in [39].

5. The stochastic model

The spatio-temporal data will be indexed by two indices; an index x to denote spatial location with $x = 1, 2, \ldots, X = 153$ and an index t to denote a point in time with $t = 1, 2, \ldots, T = 530$ for monthly maximum data. The structure of the basic model, as well as a revised model for log-transformed data and an extended model with a regression block, will be outlined below.

5.1. Basic model

The basic model is similar to the model presented in [37], inspired by [28], and contains an observation model and several state models, as outlined below. All the stochastic terms introduced in the model are assumed mutually independent and independent in space and time, having a zero-mean Gaussian distribution with some random, but identical variance, i.e., with generic notation, $\varepsilon_\beta(x,t) \overset{i.i.d}{\sim} N(0, \sigma_\beta^2)$. It should be understood that the model is defined $\forall\, x \geq 1, t \geq 1$, as relevant for each component.

At the first level, the observations (monthly maximum significant wave height), Z at location x and time t, are modelled in the observation model as the latent variable, H, corresponding to the underlying significant wave height process, and some random noise, ε_z, which may be construed as statistical measurement error:

$$Z(x,t) = H(x,t) + \varepsilon_z(x,t) \tag{1}$$

The underlying process for the significant waveheight at location x and time t is modelled by the following state model, which is assumed split into a time-independent component, $\mu(x)$, a time- and space-dependent component $\theta(x,t)$ and spatially independent seasonal, $M(t)$, and long-term trend, $\mathrm{T}(t)$, components as shown in eq. 2. The long-term temporal trend is

assumed spatially invariant and is, in fact, the component of most interest as it models the effect of climate change on the ocean wave climate.

$$H(x,t) = \mu(x) + \theta(x,t) + M(t) + \mathrm{T}(t) \tag{2}$$

The time-independent part is modelled as a first-order Markov Random Field (MRF), conditional on its nearest neighbours in all cardinal directions, and with different dependence parameters in lateral and longitudinal direction, as shown in eq. 3, with x^D = the location of the nearest gridpoint in direction D from x, where $D \in \{N, S, W, E\}$ and N = North, S = South, W = West and E = East. If x is at the border of the area, the value at the corresponding neighboring gridpoint outside the data area is taken to be zero.

$$\begin{aligned}\mu(x) = \mu_0(x) &+ a_\phi \left\{ \mu(x^N) - \mu_0(x^N) + \mu(x^S) - \mu_0(x^S) \right\} \\ &+ a_\lambda \left\{ \mu(x^E) - \mu_0(x^E) + \mu(x^W) - \mu_0(x^W) \right\} + \varepsilon_\mu(x)\end{aligned} \tag{3}$$

a_ϕ and a_λ are spatial dependence parameters in lateral (i.e. north-south) and longitudinal (i.e. east-west) direction respectively. The spatially specific mean, $\mu_0(x)$, is modelled as having a quadratic form with an interaction term in latitude and longitude. Letting $m(x)$ and $n(x)$ denote the longitude and latitude of location x respectively, it is assumed that

$$\mu_0(x) = \mu_{0,1} + \mu_{0,2} m(x) + \mu_{0,3} n(x) + \mu_{0,4} m(x)^2 + \mu_{0,5} n(x)^2 + \mu_{0,6} m(x) n(x) \tag{4}$$

The spatio-temporal dynamic term $\theta(x,t)$ is modelled as a vector autoregressive model of order one, conditionally specified on its nearest neighbours in all cardinal directions, as shown in eq. 5.

$$\begin{aligned}\theta(x,t) = b_0 \theta(x,t-1) &+ b_N \theta(x^N, t-1) + b_E \theta(x^E, t-1) \\ &+ b_S \theta(x^S, t-1) + b_W \theta(x^W, t-1) + \varepsilon_\theta(x,t)\end{aligned} \tag{5}$$

b_0 as well as the parameters corresponding to the nearest neighbours, b_N, b_E, b_S, b_W are assumed invariant in space and are assumed to have interpretations connected to the underlying sea state dynamics.

The temporal component is modelled with a seasonal and a long-term trend part. The seasonal part is modelled as an annual cyclic contribution independent of space, see eq. 6. It has also been tried to include the second harmonic to account for semi-annual seasonal contributions, but these were found to be small compared to the annual contribution, as explained in [39].

$$M(t) = c \cos(\omega t) + d \sin(\omega t) + \varepsilon_m(t) \tag{6}$$

The long-term trend of the basic model is modelled as a simple Gaussian process with a quadratic trend, as shown in eq. 7. In [37], various model alternatives were suggested for this component, i.e. with linear and quadratic trends, but in this chapter, only the results pertaining to the linear models will be considered (model alternative 2 in [37]).

$$\mathrm{T}(t) = \gamma t + \eta t^2 + \varepsilon_\mathrm{T}(t) \tag{7}$$

5.2. Revised model for log-transformed data

With the log-transformed data, denoting $Z(x,t)$ the significant wave height at location x and time t, the log-transforms are first carried out for each location and time-point ([39]),

$$Y(x,t) = \ln Z(x,t) \tag{8}$$

Then, at the observation level, the log-transformed data, Y, are modelled as the latent (or hidden) variables, H, corresponding to some underlying significant wave height process, and some random noise, ε_Y:

$$Y(x,t) = H(x,t) + \varepsilon_Y(x,t) \tag{9}$$

An equivalent representation of the observation model would be

$$Z(x,t) = e^{H(x,t)} e^{\varepsilon_Y(x,t)} \ , \tag{10}$$

where now the noise term has become a multiplicative factor rather than an additive term and, conditioned on $H(x,t)$, the significant wave height $Z(x,t)$ will be log-normally distributed.

The underlying process for the significant wave height at location x and time t is modelled by the state model which is identical to the state model for the basic model in the preceding section, but it corresponds to the alternative representation in eq. 11 on the original scale; the significant wave height can be written as the product of five multiplicative factors and therefore, the contribution from each of the model components will have a fundamentally different interpretation compared to the model for the original data.

$$Z(x,t) = e^{\mu(x)} e^{\theta(x,t)} e^{M(t)} e^{\mathrm{T}(t)} e^{\varepsilon_Y(x,t)} \tag{11}$$

In particular, the long-term trend will be modelled as a multiplicative factor, meaning that a higher trend will be ascribed to more severe sea states, i.e. extremes will be modelled with a higher trend than non-extremes. This feature was also reported by e.g. [49].

The same model alternatives as for the basic model have been tried out, but in this chapter, again only the results pertaining to the linear model will be reported.

5.3. Extended model with a regression component

Having established the basic model and found it to perform well for the significant wave height data, a model extention is introduced, where the long-term trend component $\mathrm{T}(t)$ in eq. 7 is replaced by the regression component in eq. 12 ([38]).

$$\mathrm{T}(t) = \gamma G(t) + \eta \ln G(t) + \delta G(t)^2 + \varepsilon_{\mathrm{T}}(t) \tag{12}$$

With this model, the long-term trend in monthly maximum significant wave height is regressed on CO_2 concentrations in the atmosphere, assuming first a combination of a linear, square and logarithmic trend with respect to the level of CO_2. $G(t)$ denotes the average level of CO_2 in the atmosphere at time t. It is noted that CO_2 is known to mix well in the atmosphere, so there are no spatial description of this regression term. Different alternatives

for the stochastic relationship were tried out in [38], but in this chapter only results pertaining to the model alternative performing best will be presented, i.e. the model with a combination of a linear and logarithmic relationship (setting $\delta = 0$).

5.4. Critical assumptions and prior distributions

The models presented in this chapter are stochastic models and as such they are simplified representations of the real world. All models imply simplifications and rely on a set of critical assumptions. The validity of those assumptions determines how well the model describes reality, and it is important to be aware of the most crucial model assumptions.

All the models presented in this chapter consist of different components in space and time, and an implicit assumption is that this separation of the significant wave height process into different contributions is reasonable. For example, this means that all long-term trends can be described by the separate long-term component. Also, the assumption of independent Gaussian noise associated with the various components is essential to the statistical model, but this assumption can be checked by way of normal probability plots of the residuals.

The extended model uses a regression component towards CO_2 to describe long-term variation in the ocean wave climate. Hence, a very critical model assumption is the stochastic dependence between levels of CO_2 in the atmosphere and the ocean wave climate. It is assumed that there is such a stochastic dependence and this might be a realistic assumption, as increased levels of CO_2 in the atmosphere are associated with higher temperatures, more energy in the weather systems and consequently rougher wave climate. However, it is further assumed that this stochastic dependence structure will remain essentially unchanged over time, from the past into the future. This is of course a critical assumption inherent in the model and any results are conditional on this assumption being realistic.

Furthermore, it is assumed that the CO_2 projections are reliable and results are conditional on the CO_2 data that has been utilized. In particular, no particular attention has been drawn towards possible climate tipping points or other effects that may skew the correlation between CO_2 levels in the atmosphere and ocean waves, and this introduces considerable uncertainty that has not been accounted for. Notwithstanding, the models presented herein are still believed to be interesting to investigate and they explore future ocean wave climate based on the best available knowledge of the future levels of CO_2 as a result of various emission scenarios.

Only CO_2 levels in the atmosphere have been considered, as a proxy of the level of greenhouse gases. It is normally considered that this is the dominant greenhouse gas, but omitting all other contributions is obviously a simplification. Furthermore, aerosols and other mitigating factors have not been considered as well as variability in solar radiation and external forcing.

It is noted that the model presented herein is a purely stochastic model, concerned with the stochastic dependencies in space and time, and the physics and regional characteristics of the wave climate are not modelled explicitly. However, it is argued that the physics underlying the wave generation process and all regional features are inevitably implicit in the data, and when applying the model on a particular data set any such physics and regional features

would unavoidably be incorporated by way of the data. It is noted that the models can easily be updated to account for any known biases in the data.

Informative priors have been used in a Bayesian setting, where prior knowledge has been taken into account. Conditionally conjugate priors were adopted for each model parameter. For further details and exact values of the hyperparameters used for the priors, reference is made to [37–39]. However, it is argued that the results are not overly sensitive to the chosen prior distributions. It is well known in Bayesian analysis that the priors become asymptotically irrelevant as the amount of data increases, and the amount of data is quite large in this case.

5.5. Model comparison and prediction losses

Loss functions based on predictive power were constructed in order to compare model alternatives. Only one-step predictions are considered; the models are fitted with all data except for the last timepoint and predictions of the spatial field at this timepoint are compared to the data. The standard loss function in eq. 13 is defined where, for the timepoint selected for prediction, $Z(x)$ denotes the data at location x and $Z(x)_j^*$ denotes the predicted value of Z at location x in iteration j of the MCMC simulations.

$$L_s = \left[\frac{1}{Xn} \sum_{x=1}^{X} \sum_{j=1}^{n} \left(Z(x) - Z(x)_j^* \right)^2 \right]^{\frac{1}{2}} \tag{13}$$

One alternative loss function where the squared prediction errors have been weighted according to the actual observed significant wave height is also employed. A weight of size $Z(x)$ is included in order to give greater emphasis on prediction errors at locations where large significant wave heights are observed. Hence, an alternative loss function as given in eq. 14 is calculated.

$$L_a = \left[\frac{1}{n \sum_x Z(x)} \sum_{x=1}^{X} \sum_{j=1}^{n} Z(x) \left(Z(x) - Z(x)_j^* \right)^2 \right]^{\frac{1}{2}} \tag{14}$$

The predictions $Z(x)_j^*$ are taken as the estimated value of $\boldsymbol{Z}$ given the samples for all model parameters and variables in iteration j. The model specification gives

$$Z(x)_j^* = \mu(x)_j + \theta(x,t)_j + M(t)_j + \mathrm{T}(t)_j + \varepsilon_z(t)_j \tag{15}$$

for the basic and extended models and

$$Z(x)_j^* = e^{\mu(x)_j + \theta(x,t)_j + M(t)_j + \mathrm{T}(t)_j + \varepsilon_Y(x,t)_j} \tag{16}$$

for the revised model for log-transformed data. The subscripts $_j$ denote the sampled parameters in iteration j. When using log-transformed data, the predictions are retransformed back to the original scale before the loss functions are calculated, i.e. the losses are on the same scale and should in principle be comparable although it is acknowledged that the comparison might not be completely fair for predictions made on a transformed scale.

6. Simulation results: trends and future projections

Posterior estimates of the parameters of the various models presented above have been obtained by Markov chain Monte Carlo methods, using the Gibbs sampler with additional Metropolis-Hastings steps (see e.g. [30]). Normal probability plots of the residuals indicate that the Gaussian model assumption is reasonable, and different informal tests suggest that the samples are from the stationary distribution, i.e. that the Markov chains have converged satisfactorily. Detailed results pertaining to all model components and posterior parameter estimates (mean and standard deviation), as well as descriptions of the MCMC settings, are presented in [37–40]. In this chapter, however, the main focus is on results pertaining to the long-term trends and expected future projections as a result of climate change.

6.1. Basic model

The basic model is found to perform reasonably well on the monthly maximum significant wave height data, with posterior estimates of the mean spatial field, $\mu(x)$, ranging from 6.1 to 7.3 meters over the area. The variability was greater in the north-south direction than in the east-west direction, which is reasonable. The expected contributions from the space-time dynamic part, $\theta(x,t)$ were between -1.1 and 1.8 meters and the expected seasonal contributions correspond to an annual cyclic variation of about $\pm$ 2.5 meters.

The component of most interest in this chapter, however, is the contribution from the long-term trend component $\mathrm{T}(t)$, which is included to model any long-term effects, possibly related to global climate change. According to the linear model, an expected increase in monthly maximum significant wave height of 69 cm is estimated over the data-period. The 90% credible interval ranges from 45 - 94 cm, i.e. the complete interval is positive. These posterior trend contributions are illustrated in figure 6. The black line corresponds to the mean sampled $\mathrm{T}(t)$, whereas the red lines correspond to the expected contribution γt as well as the 90% credible interval of the mean. The green line corresponds to no trend and it is clearly seen that the model detects a significant increasing trend in the wave climate.

In order to estimate future changes of the wave climate, possibly due to climate change, the estimated linear trend is extrapolated towards the year 2100. Hence, assuming that the identified long-term trend persists over 100 years, this would correspond to an expected increase in monthly maximum significant wave height of 1.6 meters over 100 years, with a 95% credibility of an increase of at least 1.0 meter.

6.2. Revised model - log-transformed data

Also the revised model, applied on the log-transformed data, seems to perform rather well on the monthly maximum data. The normal probability plots of the residuals suggest that the model revision is an improvement compared to the basic model, but the estimated losses are somewhat greater.

The expected contributions from the $\mu(x)$-field are between 1.76 and 1.95, but the interpretation is different. $e^{\mu(x)}$ is now a multiplicative factor for the monthly maximum significant wave height at location x, varying between 5.8 and 7.0 over the area. The mean

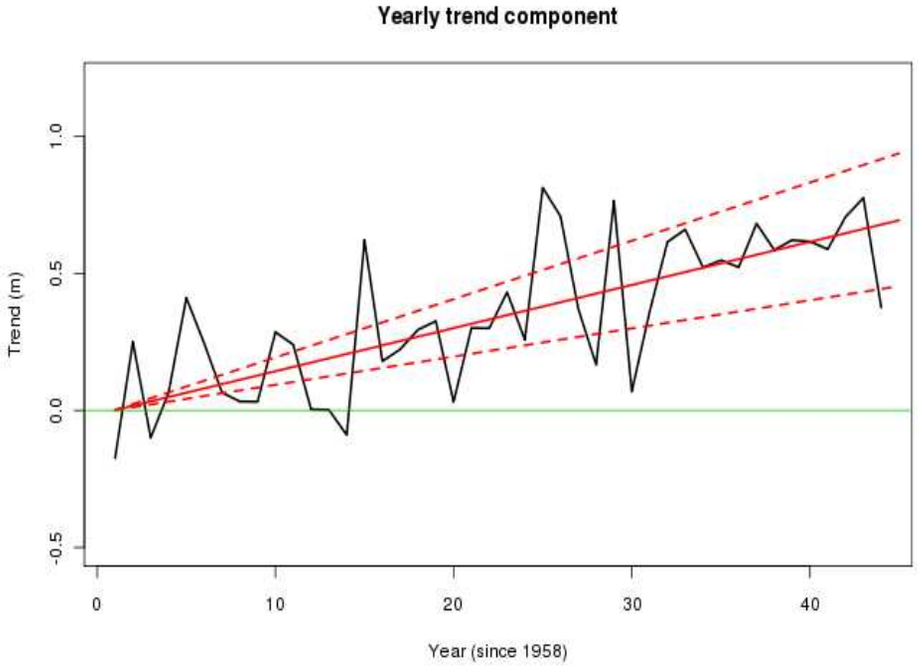

Figure 6. Estimated temporal trends of the North Atlantic wave climate; basic model

contributions from the space-time dynamic part, $\theta(x,t)$ corresponds to factors between 0.70 and 1.4 for different times and locations. Hence, this component contributes from -30% to +40%. The seasonal component corresponds to a factor 0.68 for calm seasons and 1.5 in rough seasons.

The mean estimated long-term trend from the linear model corresponds to a factor about 1.07 over the data-period. The 90% credible interval ranges from 1.03 to 1.12. For typical monthly maximum significant wave heights of, say, 5 and 8 meters respectively, this corresponds to expected increases of about 36 and 57 cm. However, for more extreme sea states, say significant wave heights of 10 or 15 meters respectively, corresponding expected increases would be 70 cm and more than 1 meter respectively. Overall, these trends are somewhat smaller than the trends estimated from the non-transformed data, but the trends pertaining to extreme conditions are greater. A QMLE-estimate for bias correction ([18]) due to retransformation has been adopted and is incorporated into the estimates above, see [39]. The estimated expected long-term trends with 90% credible interval are shown in figure 7 on the original, i.e. re-transformed scale.

Also the estimated trends obtained from the log-transformed data were extrapolated in order to obtain an estimate of future trends in the wave climate. Over 100 years, the expected future increase in monthly maximum wave height corresponds to a factor of 1.15, with a 95% credibility of a trend factor larger than 1.04. Assuming such trends to persist and valid for average monthly maximum sea states of 5 and 8 meters in calm and rough seasons, the expected increase is about 75 cm and 1.2 meters respectively. However, for more extreme sea states, with significant wave height of, say, 10 and 15 meters, expected increases would be 1.5 and 2.3 meters respectively towards the year 2100.

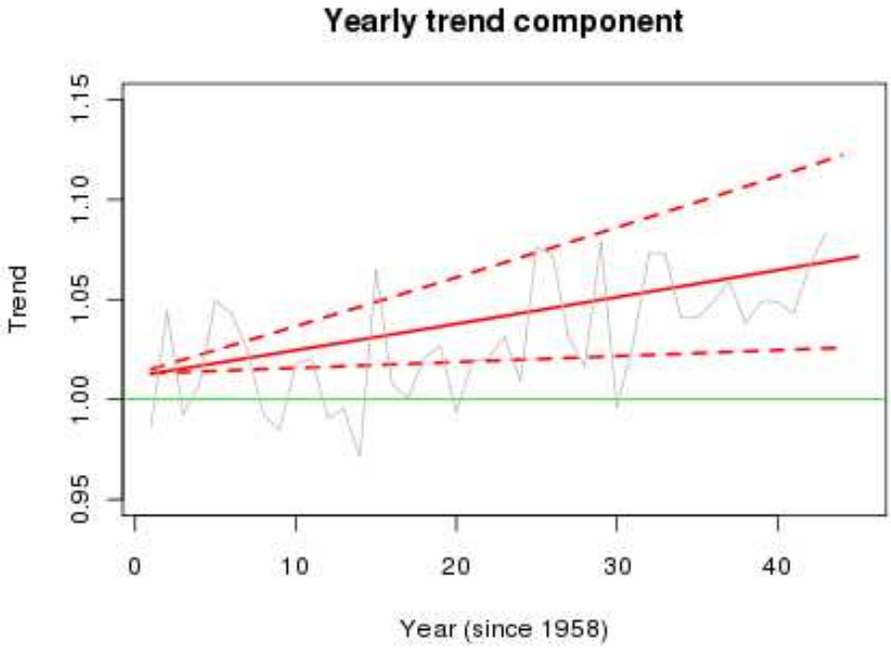

Figure 7. Estimated temporal trends of the North Atlantic wave climate; log-transformed model

6.3. Extended model with regression component

With the extended model, the stochastic relationship between significant wave height and atmospheric levels of CO_2 is exploited together with future projections of CO_2 trends in order to obtain estimates of future trends in the wave climate. Expectantly, the estimated trends should be similar to the trends estimated with the basic model, but future projections can be obtained from various CO_2 projections and may differ from the extrapolated linear trends.

It is noted that for the extended model, the long-term trend contribution does not necessarily start at 0 for t=0, but in the results presented herein, necessary adjustments have been made so that the long-term trend effectively starts at 0. For extracting the expected trends over the period 1958-2001, the long-term trend is adjusted to be 0 in 1958 and for the future projections towards 2100, the trend contribution is adjusted to start at 0 in 2001. This does not affect the relative trend between two points in time, but is accompanied by a similar but opposite adjustment of the mean spatial field.

The contributions from the adjusted time-independent field, $\mu(x)$, varies between 6.3 and 7.5 meters over the area, and this is in reasonable agreement to the estimates obtained from the basic model. The short-term dynamic contribution from $\theta(x,t)$ varies from -1.1 to 1.9 meters and the mean seasonal contributions lie between $\pm$ 2.66 meters, which also agrees well with the estimates obtained from the basic model.

The contribution from the long-term trend, possibly due to climate change, is shown in figure 8, corresponding to an expected increase of 59 cm over the period. This is somewhat lower than the estimated trend from the basic model, but still agrees fairly well. The 90% credible interval ranges from 16 to 92 cm increases in monthly maximum significant wave height.

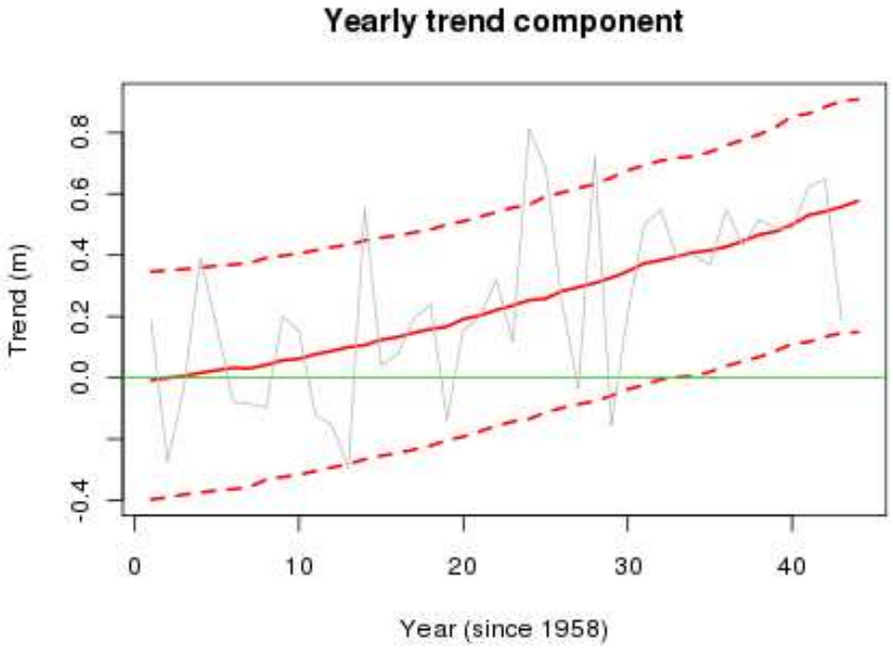

Figure 8. Estimated temporal trends of the North Atlantic wave climate; model with CO_2 regression

One of the main motivations for including the CO_2 regression component into the model was to facilitate future projections. Hence, projections of future significant wave heights are made from two future scenarios for CO_2 levels, referred to as the A2 and B1 scenario respectively. The corresponding projected trends of significant wave height are illustrated in figure 9, and it can be seen that scenario A2 yields future projections corresponding to an increase of 5.4 meters and the B1 scenario corresponds to an increase of 1.9 meters towards 2100 compared to the year 2001. The large difference between the two projections is due to the different CO_2 levels projected by the two scenarios. However, both the projected trends are considerably larger than the one obtained from extrapolating the linear trend obtained from the basic model.

The expected future projections including 90% credible intervals are illustrated in figure 10. The credible intervals are calculated from the credible intervals of the distribution of (γ, η) and do not include the uncertainty due to ε_T. For scenario A2, the 90% credible interval at year 2100 corresponds to increases in monthly maximum significant wave height over the 21 century ranging from 2.7 meters to 8.1 meters. For scenario B1, the corresponding credible interval covers a range between 1.2 to 2.6 meters increase from 2001 to 2100.

6.4. Model comparison

A crude comparison of the different model alternatives can be carried out by comparing the resulting posterior estimates of the model parameters (see [38–40]). By doing so, it is observed that the spatial features of the model seem to be barely affected by the model alterations. Since the model extensions were only related to the temporal trend, this is reassuring. The seasonal part of the model also seems to behave similarly over the model alternatives. Hence, the main

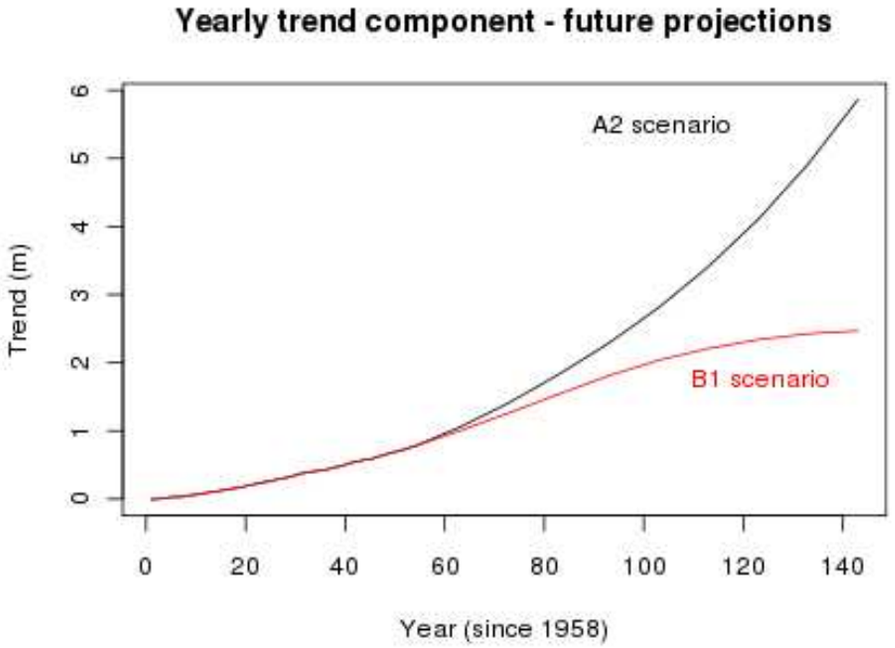

Figure 9. Estimated future trends in the North Atlantic wave climate for two emission scenarios

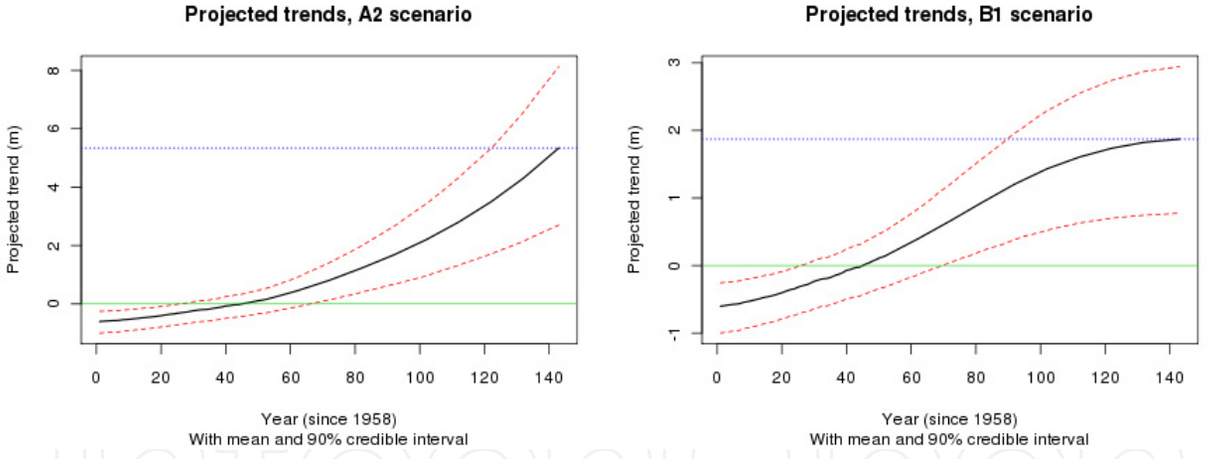

Figure 10. Estimated future trends in the North Atlantic wave climate with credible intervals

differences are, as would be expected, related to the long term temporal trend and the future projections.

The models may also be compared by way of the loss functions for short-term prediction. The estimated losses corresponding to the two loss functions for each of the model alternatives discussed herein are presented in table 2.

It is observed that both the models fitted to the original data are associated with lower losses compared to the model for log-transformed data. However, it is noted that comparison might not be fair for predictions made on log-transformed data so it does not necessarily mean that the revised model performs worst. Furthermore, the extended model with a CO_2 regression

Model alternative	L_s	L_w
Basic model	2.576	2.691
Revised model (log-transform)	3.346	3.412
Extended model (CO_2 regression)	2.562	2.674

Table 2. Model comparison: Standard and weighted loss functions

component yields the lowest losses, which indicates that this is an improvement compared to the basic model. The differences are small, however, and the estimated losses cannot be used to reliably distinguish between the models, which all seem to describe the data reasonably well.

7. Potential impact of climate change on ship structural loads

If indeed the future wave climate will become rougher, as predicted by the models presented herein, this might have an impact on the safety of maritime transportation, since ships are then likely to experience greater environmental loads. Extreme environmental loads represent a serious hazard to ship operations and any increasing trends might thus lead to higher risk, if not properly accounted for in design and operational procedures.

Having identified a trend in the significant wave height data, it would therefore be of great interest to consider how such results could be related to the calculation of future environmental loads and responses on ships and other floating structures. Trends in the ocean wave climate will obviously also be important for offshore and coastal structures, and the results can generally be applied also to offshore and coastal structures design. However, if applied to fixed installations, location specific data should be used; North Atlantic data are used only for ship design. For the purpose of this study, the trends towards 2100 estimated from the basic model and the extended model with a CO_2 regression component and scenario B1 will be assumed. It will be investigated how to relate such trends to the calculations of ship structural loads and responses. It is emphasized that potential influence of such trends on structural design, as was discussed in [8] is not considered explicitly herein. Results pertaining to any other projection period, such as 30 or 40 years ahead in time, could also easily have been used.

The trends estimated above correspond to an addition, 100 years ahead in time, with mean 1.6 meters and standard deviation 0.39 meters from the basic model and mean 1.9 meters and standard deviation 0.65 meters from the extended model adopting the B1 scenario. The mean and standard deviation of the climatic trend contribution will be denoted by μ_{ct} and σ_{ct} when stemming from the basic model and μ_{B1} and σ_{B1} when estimated by the extended model with scenario B1, respectively, i.e. an additive trend, $T \sim (\mu_\cdot, \sigma_\cdot^2)$ will be assumed.

$$\begin{array}{ll} \mu_{ct} = 1.6m & \sigma_{ct} = 0.39m \\ \mu_{B1} = 1.9m & \sigma_{B1} = 0.65m \end{array} \tag{17}$$

It is noted that the climate trend is estimated from monthly maxima although it is applied to the whole body of the H_s distribution (the marginal distribution of significant wave height). Thus the revised H_s distribution is more representative for high values of H_s. When the impact

of the trend is explored, extreme loads are considered and this makes these assumptions less troublesome; this simplification is considered acceptable for extremes but neither for fatigue calculations nor specification of operational criteria when lower sea states are of importance.

7.1. Conditional modelling of joint metocean parameters

The marginal distribution of significant wave height is normally not sufficient for load and response calculations of marine structures; the joint distribution of several metocean parameters is required. As a minimum, the joint distribution of significant wave height and wave period is needed.

The above trends were extracted from the corrected ERA-40 data (C-ERA-40) over an area in the North Atlantic. Due to lack of information about wave period in the C-ERA-40 data, the joint distribution of significant wave height and wave period used for load calculations are based on the ERA interim data set[3] for a particular location. However, that location is contained within the area considered by the C-ERA-40 data and is assumed representative for the whole area. Furthermore, main features of the C-ERA-40 and $\text{ERA}_{\text{Interim}}$ data sets are similar, and it is assumed that any bias would be similar in the two data sets. The long-term trends obtained in the present study are therefore incorporated in the established joint distribution of significant wave height and wave period based on the $\text{ERA}_{\text{interim}}$ data.

It has previously been proposed to model the marginal distribution of significant wave height, H_s, according to a 3-parameter Weibull distribution and the conditional distribution of the wave period, T, conditional on the significant wave height, as a log-normal distribution ([4, 26]). Hence, the joint distribution of significant wave height and wave period will be the product of a Weibull and a log-normal distribution given H_s (eq. 18) according to the Conditional Modelling Approach (for several met-ocean parameters see [2, 3]). The 3-parameter Weibull distribution was first applied to describe significant wave height by [29].

$$f_{H_s,T}(h,t) = f_{H_s}(h) f_{T|H_s}(t|h) \tag{18}$$

It is assumed that the trend in the significant wave height corresponds to a modified marginal distribution for the significant wave height, but that the distribution of wave period, conditional on the significant wave height, remains unchanged. It is noted that even though the conditional distribution is assumed unchanged, the marginal distribution of the wave period will obviously change, so this assumption seems reasonable.

The 3-parameter Weibull distribution is parametrized by the parameters γ (location), α (scale) and β (shape), as shown in eq. 19.

$$f(x) = \frac{\beta}{\alpha}\left(\frac{x-\gamma}{\alpha}\right)^{\beta-1} e^{-\left(\frac{x-\gamma}{\alpha}\right)^{\beta}} \qquad x \geq \gamma \tag{19}$$

It is assumed that the distribution of the significant wave height after the trend has been added can be approximated by a 3-parameter Weibull distribution with the same shape parameter, i.e. that the trend can be modelled as a modification of the location and scale parameters of

[3] Website: http://www.ecmwf.int/research/era/do/get/era-interim

the 3-parameter Weibull distribution. A simulation study confirms that this is a reasonable approximation. With these assumptions, the modified parameters due to the long-term trend can be calculated so that the modified Weibull distribution has the correct expectation and variance, resulting in the modified parameters in eqs. 20-21.

$$\gamma \to \gamma' = \gamma + \mu_{ct} + \Gamma\left(\frac{1}{\beta}+1\right)\left[\alpha - \sqrt{\alpha^2 + \frac{\sigma_{ct}^2}{\Gamma\left(\frac{2}{\beta}+1\right) - \Gamma\left(\frac{1}{\beta}+1\right)^2}}\right] \tag{20}$$

$$\alpha \to \alpha' = \sqrt{\alpha^2 + \frac{\sigma_{ct}^2}{\Gamma\left(\frac{2}{\beta}+1\right) - \Gamma\left(\frac{1}{\beta}+1\right)^2}} \tag{21}$$

The 3-parameter Weibull distribution was fitted to significant wave height data for one location from the ERA-40_{Interim} data and the estimated parameters together with the modified parameters as a result of adding the projected long-term trends (over 100 years) are given in table 3. The corresponding mean and standard deviation of the distributions are also given.

	α	β	γ	E[H_s]	sd[H_s]
Fitted distribution	2.776	1.471	0.8888	3.401	1.737
Modified parameters (Basic model trend)	2.846	1.471	2.393	4.969	1.781
Modified parameters (Extended model / B1)	2.965	1.471	2.613	5.296	1.855

Table 3. Fitted and modified parameters for the 3-parameter Weibull distribution for significant wave height

It is observed that the mean of the modified distribution is changed quite drastically, whereas there is only a slight increase in the standard deviation as a result of adding the climatic trend with uncertainties.

The conditional distribution of wave period is modelled as a log-normal distribution where the parameters are modelled as functions of significant wave height, as shown in eqs. 22-23. By assumption, this conditional distribution is not expected to change due to climatic trends, and the parameters a_i and b_i for $i = 1, 2, 3$ are estimated from the data. The resulting joint densities of the original and the modified distributions for significant wave height, H_s, and zero-up-crossing period, T_z, are illustrated by the contour plots in figure 11 (on the same scale). It is noted that T_z is one of several ways of describing the wave period, T.

$$\mu_t = E[\ln T_z | H_s = h_s] = a_1 + a_2 h_s^{a_3} \tag{22}$$

$$\sigma_t = sd[\ln T_z | H_s = h_s] = b_1 + b_2 e^{b_3 h_s} \tag{23}$$

7.2. Case study: Impact of long-term trends on the load assessment of an oil tanker

As an illustrative example, load characteristics will be calculated for an oil tanker of 250 m length and 40 m width with the same characteristics as the one reported in [5].

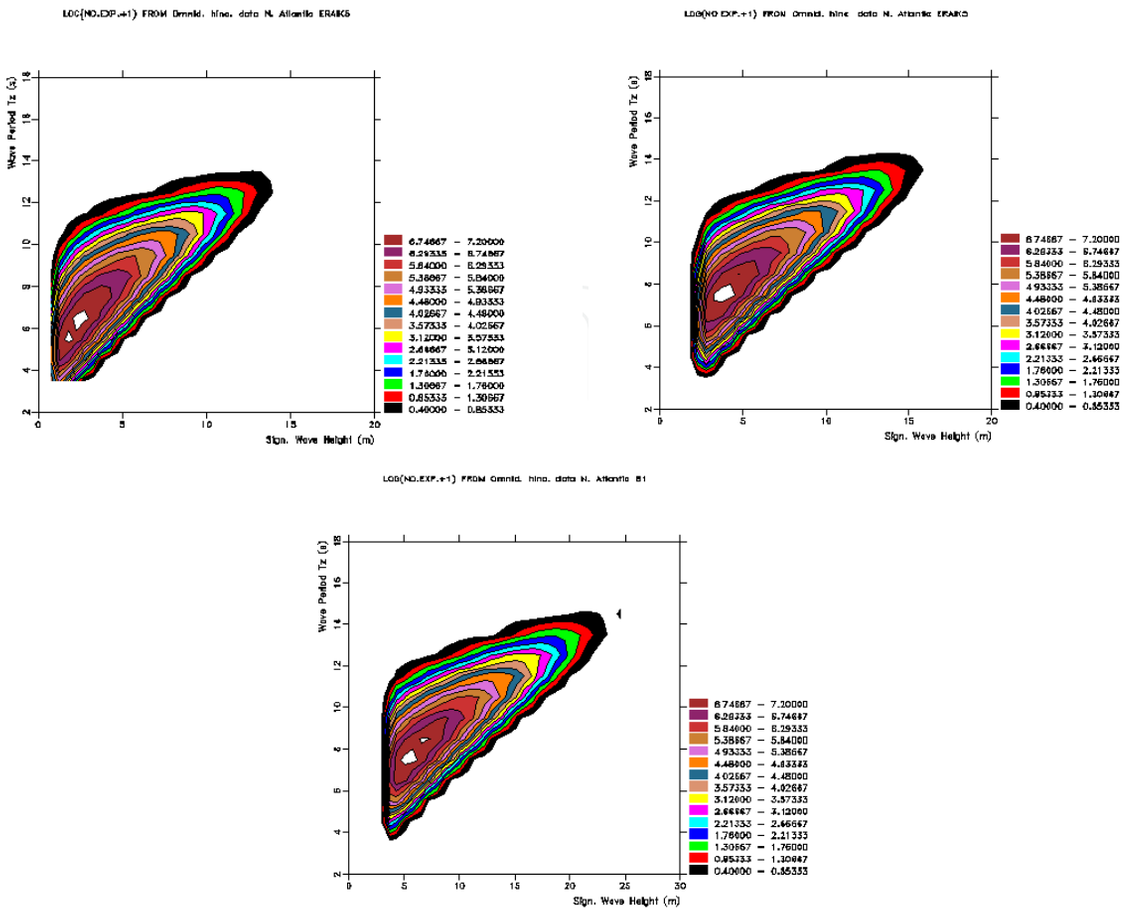

Figure 11. Contour plots of the joint distribution of significant wave height and zero-up-crossing period; Fitted distributions (top left) and modified distributions with trends estimated from the basic model (top right) and the extended model with the B1 scenario (bottom)

When specifying design criteria as well as carrying out load and response assessment for marine structures a full long-term load and response analysis can be applied, or alternatively, the environmental contour concept outlined in [48] can be used (IFORM). The latter is a valid, simplified and rational method of estimating extreme conditions and is recommended by DNV ([16]). The idea is to define contours in the environmental parameter space (usually H_s, T_z) within which extreme responses with a given return period should lie. It requires determination of the joint environmental model of sea state variables of interest. It should be noticed that the contours are found by relating sea state variables to the standard normal variables, an assumption that may affect their accuracy. Furthermore, adding the trend introduces a dependency between the sea states at subsequent times, but the effect this might have on the return values have been ignored in this study. Presumably, since the variability of the estimated trend is small in comparison to the variability of sea states, this effect is not very great.

Figure 12 shows the environmental contour lines of H_s and T_z for the North Atlantic location considered in the present study. The 1, 10, and 25-year return period levels calculated by IFORM are shown for the fit to the original $\text{ERA}_{\text{Interim}}$ data and for the corrected fits where the long-term trends are included. The 3-parameter Weibull distributions for H_s given in table 3

and the conditional log-normal distribution for T_z have been used in the analysis. As expected, the modification of the distribution for significant wave height moves the environmental contours upwards and to the right. Furthermore, the long-term trend correction has narrowed the contours and increased the maximum 1, 10 and 25-year return H_s and related T_z.

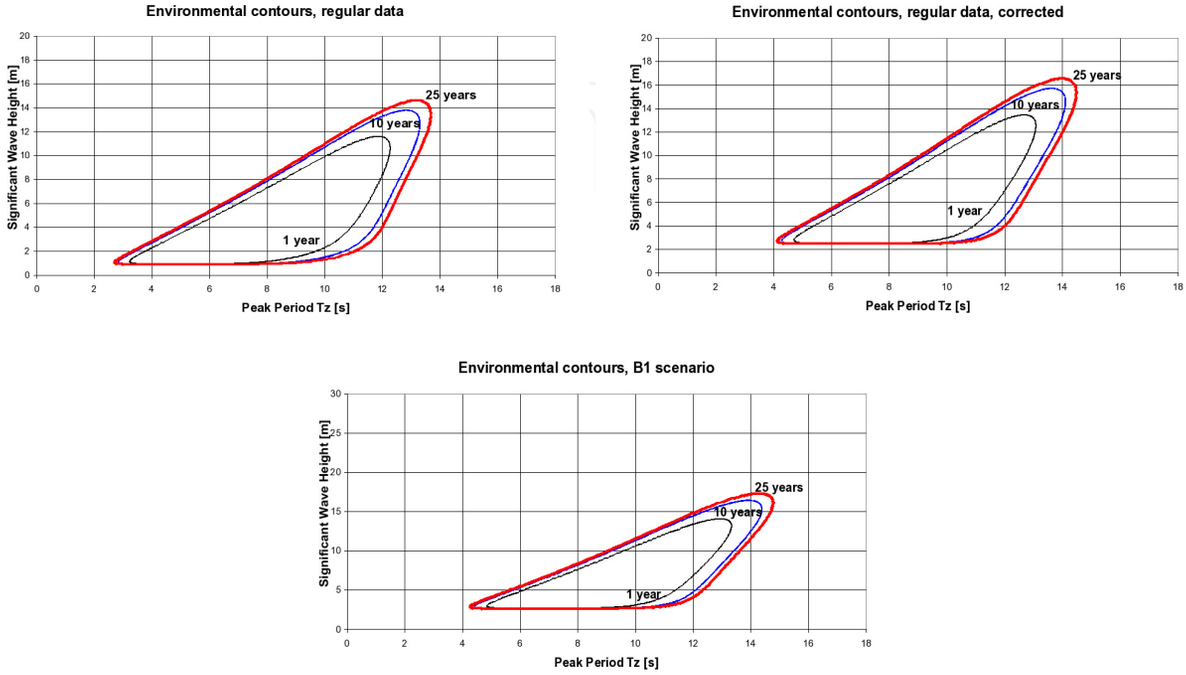

Figure 12. Environmental contour lines for the $ERA_{Interim}$ data derived from the original data (top left) and modified with the climatic trend over 100 years from the basic model (top right) and from the extended model with the B1 scenario (bottom)

The 25-year stress amplitudes for the considered oil tanker have been calculated in the 25-year sea states (H_s, T_z) given by the environmental contour lines. A 3-hour sea state duration and a Rayleigh distributed stress process in a short-term sea state (see [5]) have been assumed in the calculations. Table 4 includes the results of the analysis for the original joint (H_s, T_z) fit and the modified ones, taking the estimated 100-year long-term trends into account. The response characteristics obtained using the original (H_s, T_z) fit to the $ERA_{Interim}$ data are referred to herein as a Base Case and only relative increases in comparison to the Base Case are given in table 4.

	Stress amplitude (MPa)	Response period (s)
Base case	1.0	1.0
Modified fit - Basic model	1.07	1.02
Modified fit - Extended model / B1	1.10	1.02

Table 4. 25-year extreme load characteristics

As seen in table 4 incorporation of the long-term trend in the H_s distribution has increased the 25-year stress amplitude significantly and also the zero-crossing response period has been increased. The 25-year stress amplitude has increased by 7% or 10% while the zero-crossing response period has increased by 2% due to the estimated long-term trend over 100 years. It

is noted that similar calculations have not been done for the A2 scenario, but the effect would presumably be even larger for such a worst-case trend. Furthermore, the potential effect of the modified environmental contours on the structural loads is highly ship-dependent and even though the loads were found to increase significantly for this particular ship, it does not necessarily generalize to all types and sizes of ships.

8. Discussion

The models presented in this chapter aim at modelling the effect of climate change on the North Atlantic wave climate, and all model variations agree that the ocean wave climate has become rougher and is likely to become even rougher towards the next century. In [41], the models have been fitted to data for 11 other ocean areas around the globe with increasing trends predicted also for 9 of these.

Different emission scenarios have been assumed in the extended model to obtain different future projections of the wave climate, and it has been seen that adopting an extreme emission scenario, such as the A2 scenario, corresponds to predicting extreme future trends in significant wave height. With a more moderate emission scenario, such as B1, the resulting future projections are still larger than the extrapolation of observed recent trends, as predicted by the basic model. As for any future climate predictions, uncertainties are large and it is difficult to determine which predictions are best. According to the two loss functions utilized in this study (eqs. 13-14), the extended model seems to represent an improvement in describing the data at hand but this does not necessarily mean that the projections from this model are more reliable than the others; significant uncertainties are also related to the CO_2 scenarios proposed by IPCC. However, the extended model may adopt different CO_2 scenarios and investigate their effects on the trends in the future ocean wave climate.

An implicit assumption inherent in the extended model is that there is stochastic dependence between atmospheric CO_2 levels and the ocean wave climate, and also that this relationship will remain essentially the same in the future. It is assumed that an increase of greenhouse gases in the atmosphere will increase the temperature and put more energy into the weather systems, leading to more powerful storms and wind fields. This might again change the ocean wave climate, since it is well known that ocean waves are generated by wind and air pressure gradients. This is obviously a simplification, and it is possible to refine the model with different layers of dynamics and relationships, e.g. including projections of wind or pressure fields as explanatory variables in the model. Notwithstanding, it is argued that the physics underlying the wave generation process is inevitably implicit in the data, and when applying the models to a particular data set any such physical effects would unavoidably be incorporated by way of the data. On the other hand, the stochastic models are affected by data uncertainties and possible biases.

Comparing the projections obtained with the different Bayesian hierarchical space-time models with previous studies, it is seen that apart from the predictions pertaining to the A2 scenario, the projections are comparable to those made for the North Atlantic in e.g. [12, 14, 15, 19, 42–44]. The uncertainties are large, the estimated 90% credible intervals correspond to about $\pm$ 50% of the expected projections, and the intervals generally overlap. It should also be kept in mind that the trends predicted herein pertain to the monthly maxima

and the maxima might experience a greater change than moderate sea states, as also suggested in e.g. [49]. The A2 scenario can be construed as a worst case scenario and is important to consider from a precautionary perspective. Nevertheless, even stronger trends were predicted in [31], albeit for an area in the Pacific ocean.

It should be stressed that even though the models detect trends in the data, it does not necessarily mean that the trend is a direct consequence of anthropogenic climate change. It might be a result of decadal natural variability, as discussed in e.g. [9], and wave climate variability has been reported to be considerable on different temporal scales ([17]). Great care should therefore be taken when interpreting the meaning and the origin of this trend, even though the correlation between anthropogenic CO_2 emissions and the wave climate are found to be strong in this study.

One practical implication of the predicted changes in the ocean wave climate due to global climate change is that the structural loads and stresses on ships and other marine structures might increase notably in the future. A case study indicates increases of up to 10% over the current century. This is not negligible, and it is therefore recommended to carefully consider and take into account the potential impact of climate change in the design and construction of ocean going ships to avoid jeopardizing the safety of future maritime operations.

9. Conclusions

This chapter has been concerned with the potential impact of global climate change on the ocean wave climate and, consequently, on the risk of maritime transportation. A Bayesian hierarchical space-time model that has been developed to model the effect of climate change on the ocean wave climate has been presented. Different versions of the model have been discussed and they all agree in a non-negligible positive trend in the monthly maximum significant wave height over a selected area of the North Atlantic ocean. Estimated expected additive trends towards 2100 range from 1.6 - 5.4 meters and expected multiplicative trends in the order of 15% are predicted. Assuming an average monthly maximum significant wave height of 7.5 meters, the estimated trends related to the B1 and A2 scenarios correspond to centurial increases of 25% - 72%, which are indeed significant. However, the uncertainties are large, and 90% credible intervals for the expected trends range from 1.2 to 2.6 meters for the B1 scenario and 2.7 to 8.1 meters for the A2 scenario.

One of the advantages of using a stochastic model is that estimates of the uncertainties are given explicitly. These are important when future projections are to be incorporated in risk analyses or utilized in probabilistic load calculations as illustrated by an example in this chapter. The case study reveals that the effect of the predicted trend in the ocean wave climate on environmental loads of ships is far from being negligible, and that this may need to be taken into account in design and construction of ships. Obviously, a roughening of the ocean wave climate also has the potential to severely impact other areas of society as well, related to maritime, offshore and coastal activities. Combined with sea level rise and other possible effects of climate change, coastal areas throughout the globe may be seriously affected.

How to adapt to climate change is one of the most important questions in society today. It is a political question and perhaps a moral question as much as it is a scientific

question. Nevertheless, an important prerequisite for making well-founded decisions is reliable predictions of the future effect of climate change. The stochastic model presented in this chapter aims at contributing to this discussion by providing a model for predicting the effect of climate change on the ocean wave climate. Such an effect could again have practical implications on many areas of society, most notably related to marine and coastal management. It is acknowledged that the models represent a simplification of reality, as inevitably all models do, and that there is potential for improvements to the models. Nonetheless, it is believed that the study presented herein is an important contribution to the scientific debate on the effects of climate change, and it is a hope that it can spur further debate and motivate further research into the effects of climate change on the future ocean wave climate.

Acknowledgments

The authors want to express their thanks to Dr. Andreas Sterl at KNMI for kindly providing the significant wave height data used in this analysis and for clarifying some issues discovered when investigating the data. Thanks also to Dr. Pieter Tans for kind permission to use the NOAA ESRL CO_2-data. Furthermore, thanks to the Norwegian Meteorological Institute for providing the $ERA_{Interim}$ data. The data on future projections of atmospheric concentration of CO_2 were obtained from the IPCC.

Author details

Erik Vanem, Bent Natvig and Arne Bang Huseby
University of Oslo, Norway

Elzbieta M. Bitner-Gregersen
Det Norske Veritas, Norway

10. References

[1] Arena, F. & Pavone, D. [2009]. A generalized approach for long-term modelling of extreme crest-to-trough wave heights, *Ocean Modelling* 26: 217–225.

[2] Bitner-Gregersen, E. & Haver, S. [1989]. Joint long term description of environmental parameters for structural response calculation, *Proc. 2nd International Workshop on Wave Hindcasting and Forecasting*.

[3] Bitner-Gregersen, E. & Haver, S. [1991]. Joint environmental model for reliability calculations, *Proc. 1st International Offshore and Polar Engineering conference (ISOPE 1991)*, The International Society of Offshore and Polar Engineering (ISOPE).

[4] Bitner-Gregersen, E. M. [1988]. Appendix: Joint long term distribution of Hs, Tp, *Probabilistic Calculation of Design Criteria for Ultimate Tether Capacity of Snorre TLP*, Madsen, H.O., Rooney, P. and Bitner-Gregersen, E. Det Norske Veritas Report No. 87-31.

[5] Bitner-Gregersen, E. M., Cramer, E. H. & Løseth, R. [1995]. Uncertainties of load characteristics and fatigue damage of ship structures, *Marine Structures* 8: 97–117.

[6] Bitner-Gregersen, E. M. & de Valk, C. [2008]. Quality control issues in estimating wave climate from hindcast and satellite data, *Proc. 27th International Conference on*

Offshore Mechanics and Arctic Engineering (OMAE 2008), American Society of Mechanical Engineers (ASME).

[7] Bitner-Gregersen, E. M. & Hagen, Ø. [1990]. Uncertainties in data for the offshore environment, *Structural Safety* 7: 11–34.

[8] Bitner-Gregersen, E. M., Hørte, T. & Skjong, R. [2011]. Potential impact of climate change on tanker design, *Proc. 30th International Conference on Ocean, Offshore and Arctic Engineering (OMAE 2011)*, American Society of Mechanical Engineers (ASME).

[9] Caires, S. & Sterl, A. [2005a]. 100-year return value estimates for ocean wind speed and significant wave height from the ERA-40 data, *Journal of Climate* 18: 1032–1048.

[10] Caires, S. & Sterl, A. [2005b]. A new nonparametric method to correct model data: Application to significant wave height from ERA-40 re-analysis, *Journal of Atmospheric and Oceanic Technology* 22: 443 – 459.

[11] Caires, S. & Swail, V. [2004]. Global wave climate trend and variability analysis, *Preprints of 8th International Workshop on Wave Hindcasting and Forecasting*.

[12] Caires, S., Swail, V. R. & Wang, X. L. [2006]. Projection and analysis of extreme wave climate, *Journal of Climate* 19: 5581–5605.

[13] Cressie, N. & Wikle, C. K. [2011]. *Statistics for Spatio-Temporal Data*, Wiley.

[14] Debernard, J. B. & Røed, L. P. [2008]. Future wind, wave and storm surge climate in the Northern Seas: a revisit, *Tellus* 60A: 427–438.

[15] Debernard, J., Sætra, Ø. & Røed, L. P. [2002]. Future wind, wave and storm surge climate in the northern North Atlantic, *Climate Research* 23: 39 – 49.

[16] DNV [2010]. *Environmental Conditions and Environmental Loads*, Det Norske Veritas. DNV-RP-C205.

[17] Dodet, G., Bertin, X. & Tabora, R. [2010]. Wave climate variability in the North-East Atlantic Ocean over the last six decades, *Ocean Modelling* 31: 120–131.

[18] Ferguson, R. [1986]. River loads underestimated by rating curves, *Water Resources Research* 22: 74–76.

[19] Grabemann, I. & Weisse, R. [2008]. Climate change impact on extreme wave conditions in the North Sea: an ensemble study, *Ocean Dynamics* 58: 199 – 212.

[20] IPCC [2001]. *Climate Change 2001: The Scientific Basis*, Cambridge University Press.

[21] IPCC [2007a]. Climate change 2007: Synthesis report, *Technical report*, Intergovernmental Panel on Climate Change.

[22] IPCC [2007b]. *Climate Change 2007: The Physical Sciences Basis. Contribution of Working Group I to the Fourth Assessment Report of the Intergovernmental Panel on Climate Change*, Cambridge University Press.

[23] IPCC [2012]. *Managing the Risks of Extreme Events and Disasters to Advance Climate Change Adaptation*, Cambridge University Press.

[24] Jain, A. K., Kheshgi, H. S. & Wuebbles, D. J. [1994]. Integrated science model for assessment of climate change, *Technical Report UCRL-JC-116526*, Lawrence Livermore National Laboratory.

[25] Kheshgi, H. S. & Jain, A. K. [2003]. Projecting future climate change: Implications of carbon cycle model intercomparisons, *Global Biogeochemical Cycles* 17: 1047.

[26] Mathisen, J. & Bitner-Gregersen, E. [1990]. Joint distributions for significant wave height and wave zero-up-crossing period, *Applied Ocean Research* 12: 93–103.

[27] Nakićenović, N., Alcamo, J., Davis, G., de Vries, B., Fenhann, J., Gaffin, S., Gregory, K., Grügler, A., Jung, T. Y., Kram, T., La Rovere, E. L., Michaelis, L., Mori, S., Morita, T., Pepper, W., Pitcher, H., Price, L., Riahi, K., Roehrl, A., Rogner, H.-H., Sankovski, A., Schlesinger, M., Shukla, P., Smith, S., Swart, R., van Rooijen, S., Victor, N. & Dadi, Z. [2000]. *Emissions scenarios*, Cambridge University Press.

[28] Natvig, B. & Tvete, I. F. [2007]. Bayesian hierarchical space-time modeling of earthquake data, *Methodology and Computing in Applied Probability* 9: 89–114.

[29] Nordenstrøm, N. [1973]. A method to predict long-term distributions of waves and wave-induced motions and loads on ships and other floating structures, *Technical Report 81*, Det Norske Veritas.

[30] Robert, C. P. & Casella, G. [2004]. *Monte Carlo Statistical Methods*, second edn, Springer.

[31] Ruggiero, P., Komar, P. D. & Allan, J. C. [2010]. Increasing wave heights and extreme value projections: The wave climate of the U.S. Pacific Northwest, *Coastal Engineering* 57: 539–552.

[32] Sterl, A. & Caires, S. [2005]. Climatology, variability and extrema of ocean waves: The web-based KNMI/ERA-40 wave atlas, *International Journal of Climatology* 25: 963–977.

[33] Thoning, K. W., Tans, P. P. & Komhyr, W. D. [1989]. Atmospheric carbon dioxide at Mauna Loa observatory 2. analysis of the NOAA GMCC data, 1974-1985, *Journal of Geophysical Research* 94: 8549–8565.

[34] Uppala, S. M., Kållberg, P. W., Simmons, A. J., Andrae, U., Da Costa Bechtold, V., Fiorino, M., Gibson, J. K., Haseler, J., Hernandez, A., Kelly, G. A., Li, X., Onogi, K., Saarinen, S., Sokka, N., Allan, R. P., Andersson, E., Arpe, K., Balmaseda, M. A., Beljaars, A. C. M., Van de Berg, L., Bidlot, J., Bormann, N., Caires, S., Chevallier, F., Dethof, A., Dragosavac, M., Fisher, M., Fuentes, M., Hagemann, S., Hólm, E. Hoskins, B. J., Isaksen, L., Janssen, P. A. E. M., Jenne, R., McNally, A. P., Mahfouf, J.-F., Morcrette, J.-J., Rayner, N. A., Saunders, R. W., Simon, P., Sterl, A., Trenberth, K. E., Untch, A., Vasiljevic, D., Vitebro, P. & Woolen, J. [2005]. The ERA-40 re-analysis, *Quarterly Journal of the Royal Meteorological Society* 131: 2961–3012.

[35] Vanem, E. [2011]. Long-term time-dependent stochastic modelling of extreme waves, *Stochastic Environmental Research and Risk Assessment* 25: 185–209.

[36] Vanem, E. & Bitner-Gregersen, E. [2012]. Stochastic modelling of long-term trends in the wave climate and its potential impact on ship structural loads, *Applied Ocean Research* 37: 235–248.

[37] Vanem, E., Huseby, A. B. & Natvig, B. [2012a]. A Bayesian hierarchical spatio-temporal model for significant wave height in the North Atlantic, *Stochastic Environmental Research and Risk Assessment* 26: 609–632.

[38] Vanem, E., Huseby, A. B. & Natvig, B. [2012b]. Bayesian hierarchical spatio-temporal modelling of trends and future projections in the ocean wave climate with a CO_2 regression component, submitted.

[39] Vanem, E., Huseby, A. B. & Natvig, B. [2012c]. Modeling ocean wave climate with a Bayesian hierarchical space-time model and a log-transform of the data, *Ocean Dynamics* 62: 355–375.

[40] Vanem, E., Huseby, A. B. & Natvig, B. [2012d]. A stochastic model in space and time for monthly maximum significant wave height, *Proc. Ninth International Geostatistics Congress (Geostats 2012)*: 505–517.

[41] Vanem, E., Natvig, B. & Huseby, A. B. [2012]. Modelling the effect of climate change on the wave climate of the world's oceans, *Ocean Science Journal* 47: 123–145.
[42] Wang, X. J., Zwiers, F. W. & Swail, V. R. [2004]. North Atlantic ocean wave climate change scenarios for the twenty-first century, *Journal of Climate* 17: 2368–2383.
[43] Wang, X. L. & Swail, V. R. [2006a]. Climate change signal and uncertainty in projections of ocean wave heights, *Climate Dynamics* 26: 109–126.
[44] Wang, X. L. & Swail, V. R. [2006b]. Historical and possible future changes of wave heights in northern hemisphere oceanc, *in* W. Perrie (ed.), *Atmosphere-Ocean Interactions*, Vol. 2 of *Advances in Fluid Mechanics, Vol. 39*, WIT Press, chapter 8, pp. 185–218.
[45] Wikle, C. K. [2003]. Hierarchical models in environmental science, *International Statistical Review* 71: 181 – 199.
[46] Wikle, C. K., Berliner, L. M. & Cressie, N. [1998]. Hierarchical Bayesian space-time models, *Environmental and Ecological Statistics* 5: 117 – 154.
[47] Wikle, C. K., Milliff, R. F., Nychka, D. & Berliner, L. M. [2001]. Spatiotemporal hierarchical Bayesian modeling: Tropical ocean surface winds, *Journal of the American Statistical Association* 96: 382 – 397.
[48] Winterstein, S., Ude, T., Cornell, C., Bjerager, P. & Haver, S. [1993]. Environmental parameters for extreme response: Inverse FORM with omission factors, *Proc. 6th International Conference on Structural Safety and Reliability*.
[49] Young, I., Zieger, S. & Babanin, A. [2011]. Global trends in wind speed and wave height, *Science* 332: 451–455.

IntechOpen